

# Faraday Rotation in Pulsar Magnetosphere

Chen Wang<sup>1</sup>, J. L. Han<sup>1</sup>, Dong Lai<sup>2</sup>

<sup>1</sup> *National Astronomical Observatories, Chinese Academy of Sciences. A20 Datun Road, Chaoyang District, Beijing 100012, China*

<sup>2</sup> *Department of Astronomy, Cornell University, Ithaca, NY 14853, USA*

E-mail: wangchen@nao.cas.cn

20 January 2013

## ABSTRACT

The magnetosphere of a pulsar is composed of relativistic plasmas streaming along the magnetic field lines and corotating with the pulsar. We study the intrinsic Faraday rotation in the pulsar magnetosphere by critically examining the wave modes and the variations of polarization properties for the circularly polarized natural modes under various assumptions about the magnetosphere plasma properties. Since it is difficult to describe analytically the Faraday rotation effect in such a plasma, we use numerical integrations to study the wave propagation effects in the corotating magnetosphere. Faraday rotation effect is identified among other propagation effects, such as wave mode coupling and the cyclotron absorption. In a highly symmetrical electron-positron pair plasma, the Faraday rotation effect is found to be negligible. Only for asymmetrical plasmas, such as the electron-ion streaming plasma, can the Faraday rotation effect become significant, and the Faraday rotation angle is found to be approximately proportional to  $\lambda^{0.5}$  instead of the usual  $\lambda^2$ -law. For such electrons-ion plasma of pulsar magnetosphere, the induced rotation measure becomes larger at higher frequencies, and should have opposite signs for the emissions from opposite magnetic poles.

**Key words:** polarization – radiative transfer – star: magnetic fields – pulsars: general

## 1 INTRODUCTION

Radio emissions from pulsars are generally highly polarized. When the radio waves propagate through the magneto-ionized interstellar medium (ISM), the linear polarization plane is rotated by an angle proportional to  $\int B n_e dl \cdot \lambda^2$ . This is the Faraday rotation (FR) effect. The rotation measure,  $RM = \int B n_e dl$ , can be measured from the polarization angles at different frequencies (Hamilton & Lyne 1987; Han et al. 1999, 2006).

Some questions need to be answered when pulsar rotation measures are used to investigate the properties of the interstellar medium. Do the RMs of pulsars completely come from the ISM? Is there any intrinsic Faraday rotation from pulsar magnetosphere? If so, how large is it? Because the intrinsic polarization position angles of pulsar emission vary with the pulsar rotation phase, is the RM different for different phase bin? How to average the RMs by different weights of different phases? The RMs from ISM should not vary with rotation phase. However, recent observations by Ramachandran et al. (2004) and Noutsos et al. (2009) showed that for some pulsars the observed RMs do vary with the rotation phases, indicating that the RMs do not just come from the ISM.

There are three possible reasons for the different phase-resolved RM: (1) the effect of incoherent superposition of quasi-orthogonal polarization modes of pulsar emission (Ramachandran et al. 2004); (2) interstellar scattering (Noutsos et al. 2009, Karastergiou 2009); (3) intrinsic Faraday rotation in pulsar magnetospheres. The first two possibilities have already been discussed previously, while the third has not been addressed carefully. Although Kennett & Melrose (1998) discussed the generalized Faraday rotation effect in relativistic plasmas when the natural modes are linearly polarized, they did not consider the Faraday rotation for the circularly polarized natural modes in such a plasma.

In this paper, we investigate the intrinsic Faraday rotation in pulsar magnetospheres when the natural wave modes are circularly polarized. A pulsar magnetosphere consists of highly magnetized relativistic streaming plasmas, different from the ISM. Thus, the simple  $\lambda^2$  relation for the Faraday rotation may not apply. In § 2, we give the theoretical description of the natural modes in the relativistic streaming plasma, and analyze the Faraday rotation effect. Because it is not easy to obtain analytic expression for the Faraday rotation effect for such a plasma, in § 3 we study this effect by numerically integration of the wave vectors in a self-consistent manner. Our conclusions are presented in § 4.

## 2 FARADAY ROTATION FOR CIRCULARLY POLARIZED NATURAL MODES IN PULSAR MAGNETOSPHERE

In any magnetized medium, when the natural modes are circularly polarized and the mode evolution is adiabatic, Faraday rotation effect should rotate the linear polarization position angle ( $\phi_{\text{PA}}$ ) by

$$\Delta\phi_{\text{PA}} = \int \frac{\Delta k}{2} dr. \quad (2.1)$$

Here  $\Delta k = \Delta n\omega/c$  is the wave number difference of the two circularly polarized natural modes,  $dr$  is the unit distance in photon ray <sup>1</sup>. In our previous papers (Wang & Lai 2007; Wang, Lai & Han 2010, hereafter WLH10), we have already derived the dielectric tensor and wave modes in pulsar magnetospheres composed of streaming, relativistic plasmas of various compositions and Lorentz factors. With the dielectric tensor, we can solve the Maxwell equation and obtain two eigenmodes, to be labeled as the plus “+” mode and minus “−” mode, and corresponding refractive indices  $n_{\pm}$ . We write the polarization vectors of the two modes as  $\mathbf{E}_{\pm} = \mathbf{E}_{\pm T} + \mathbf{E}_{\pm z}\hat{\mathbf{z}}$  in the  $xyz$ -frame, with  $\hat{\mathbf{z}} = \hat{\mathbf{k}}$ ,  $\mathbf{B}$  in the  $xz$ -plane and  $\hat{\mathbf{k}} \times \hat{\mathbf{B}} = -\sin\theta_B\hat{\mathbf{y}}$ . The transverse part of the mode polarization vector is given by

$$\mathbf{E}_{\pm T} = \frac{1}{(1 + K_{\pm}^2)^{1/2}}(iK_{\pm}, 1), \quad (2.2)$$

where  $iK_{\pm} = (E_x/E_y)_{\pm}$ . From the Maxwell equation and dielectric tensor, we obtain

$$K_{\pm} = \beta_{\text{pol}} \pm \sqrt{\beta_{\text{pol}}^2 + 1}, \quad (2.3)$$

with the polarization parameter

$$\beta_{\text{pol}} \simeq -\frac{f_{\eta} \sin^2 \theta_B u_r^2 / (1 - u_r^2)}{2\Sigma_s f_{12,s} (\cos \theta_B - \xi_s \sin \theta_B)}. \quad (2.4)$$

Here  $f_{\eta}$ ,  $f_{12,s}$ ,  $\xi_s$  are factors in dielectric tensor [see eqs. (3.15) and (3.16) of WLH10], the sum  $\Sigma_s$  runs over each charged particle species “s” (electrons, positrons and/or ions). The dimensionless parameter  $u_r = \omega_c / [\gamma\omega(1 - \beta \cos \theta_B)]$  stands for the ratio of cyclotron frequency  $\omega_c$  and the rest-frame frequency  $\gamma\omega(1 - \beta \cos \theta_B)$ , with  $\omega$  the wave frequency,  $\gamma$  the Lorentz factor of streaming plasma, and  $\theta_B$  the  $\mathbf{k}$ - $\mathbf{B}$  angle. Obviously, when  $|\beta_{\text{pol}}| \gg 1$ , the two eigenmodes are linearly polarized, while for  $|\beta_{\text{pol}}| \ll 1$  the two modes are circularly polarized ( $K_{\pm} = \pm 1$ ). The refractive indices of the two modes can be written as

$$n_{\pm}^2 = 1 + f_{11} \pm K_{\pm} \Sigma_s f_{12,s} (\cos \theta_B - \xi_s \sin \theta_B). \quad (2.5)$$

<sup>1</sup> In this paper,  $r$  stands for the distance from the neutron star center. Since the emission and propagation regions are far away from the NS surface, we do not distinguish the small difference of  $dr$  between the photon ray and radial direction.

Since  $n_{\pm}$  is very close to the unity, the difference between the two refractive indices can be written as

$$\Delta n \simeq \sqrt{1 + \beta_{\text{pol}}^2} \Sigma_s f_{12,s} (\cos \theta_B - \xi_s \sin \theta_B). \quad (2.6)$$

If the electrons and positrons in the plasma are purely symmetrical in density and velocity, then the denominator of eq. (2.4) equals zero and  $\beta_{\text{pol}} = \infty$  along the photon ray; this means that the two natural modes are always linearly polarized. However, in reality there always exists some asymmetry between electrons and positrons in the pulsar magnetosphere. For example, in the Goldreich-Julian magnetosphere model (Goldreich & Julian 1969), there exists a net charge density, called Goldreich-Julian density,  $N_{\text{GJ}}$ , which specifies the density difference between electrons and positrons. Ions (such as  $\text{H}^+$  or Fe ions) may also exist in the magnetosphere. Since the interaction between ions and photons is much weaker than that between electrons/positrons and photons, the existence of ions enhances the asymmetry of the plasma. The Lorentz factors of electrons and positrons may also be different because of different electric field acceleration (Arons 1983; Kazbegi et al. 1991). If the asymmetry between electrons and positrons is sufficiently large, even though the natural modes in the inner magnetosphere of pulsars are linearly polarized, when the photons propagate to the outer magnetosphere, the natural modes could become elliptically or circularly polarized.

In this paper, for simplicity we consider a cold pair plasma, in which electrons and positrons have the same Lorentz factors ( $\gamma_p = \gamma_e = \gamma$ ) but different densities,  $\Delta N = N_p - N_e \neq 0$ . The density difference could be Goldreich-Julian density, but we will not entirely restrict ourselves to this constraint. In this case all the equations are simplified. The polarization parameter  $\beta_{\text{pol}}$  becomes

$$\beta_{\text{pol}} = -\frac{u_r \sin^2 \theta_B \gamma^{-2}}{2(1 - \beta \cos \theta_B)(\cos \theta_B - \beta) \Delta N / N}, \quad (2.7)$$

with the plasma velocity  $\beta = 1/\sqrt{1 + \gamma^2}$  and the total plasma density  $N = N_p + N_e$ . The difference of refractive indices can also be simplified to

$$\Delta n \simeq -\sqrt{1 + \beta_{\text{pol}}^2} \frac{v \gamma^{-1} u_r}{1 + i 2 \gamma_{\text{rad}} - u_r^2} \frac{\Delta N}{N} \frac{\cos \theta_B - \beta}{1 - \beta \cos \theta_B}. \quad (2.8)$$

Here  $v = \omega_p^2 / \omega^2$  relates to the plasma frequency  $\omega_p$ , and the radiative damping parameter

$$\gamma_{\text{rad}} = \frac{4e^2 \omega_c}{3m_e c^2} \quad (2.9)$$

is important only near the cyclotron resonance and can be neglected away from the resonance. The cyclotron resonance radius  $r_{\text{cyc}}$  can be written as [see eq. (4.49) of WLH10]

$$r_{\text{cyc}}/R_* = 1.8 \times 10^3 B_{*12}^{1/3} \nu_9^{-1/3} \theta_B^{-2/3} \gamma^{-1/3}. \quad (2.10)$$

Here the magnetic field is described by  $B(r) \simeq B_*(R_*/r)^3$ ,  $R_*$  is the radius of the neutron star (usually we set  $R_* = 10 \text{ km}$ ),  $B_* = 10^{12} B_{*12} \text{ G}$  is the surface magnetic field,  $\nu = \nu_9 \text{ GHz}$  is the wave frequency, and  $r$  is the distance from the neutron star center. Typically,  $\theta_B \ll 1$ ,  $\gamma \gg 1$  and  $\theta_B \gamma \gg 1$ , equations (2.7) and (2.8) can be simplified further:

$$\beta_{\text{pol}} \simeq \frac{2u_r}{\theta_B^2 \gamma^2 \Delta N / N}, \quad (2.11)$$

$$\Delta n \simeq \sqrt{1 + \beta_{\text{pol}}^2} \frac{v \gamma^{-1} u_r}{1 - u_r^2} \frac{\Delta N}{N}, \quad (2.12)$$

where we have neglected the radiative damping term. If  $\theta_B^2 \gamma^2 \Delta N / N \gg 1$ , the natural modes could become circularly polarized even before the cyclotron resonance (where  $u_r = 1$ ), and Faraday rotation could affect the photon linear polarization angle. Before and after the cyclotron resonance (where  $u_r = 1$ ),  $\Delta n$  will change signs, while  $\beta_{\text{pol}}$  keeps the same sign. This means that the Faraday rotations to PA have opposite directions before and after cyclotron resonance.

## 2.1 Faraday rotation effect for circularly polarized natural modes

For a typical  $\theta_B$  (not so close to 0,  $\theta_B \gamma \gg 1$ ), only when  $u_r < \theta_B^2 \gamma^2 \Delta N / N$ , the eigenmodes become circularly polarized [see eq. (2.11)]. We define the radius of circularization  $r_{\text{cir}}$  by  $|\beta_{\text{pol}}(r = r_{\text{cir}})| = 1$ , so that the normal modes become circularly polarized when  $r > r_{\text{cir}}$ . According to eq. (2.11), the radius of circularization is

$$r_{\text{cir}}/R_* = 2.2 \times 10^3 B_{*12}^{1/3} P_{1s}^{-1} \nu_9^{-1/3} \theta_B^{-4/3} \gamma^{-1} (\Delta N / N)^{-1/3}. \quad (2.13)$$

For the typical parameters of a pulsar magnetosphere,  $B_* = 10^{12} \text{ G}$ ,  $P = 1 \text{ s}$ ,  $\nu = 1 \text{ GHz}$ ,  $\theta_B \sim 0.1$ ,  $\gamma = 100$ , we have  $r_{\text{cir}}/r_{\text{LC}} \sim 0.1$ . If the mode evolution is adiabatic and refractive indices difference  $\Delta n$  is large enough, the linear polarization position angle will be affected by the Faraday rotation significantly. The position angle is rotated by

$$\Delta \phi_{\text{PA}} \simeq \int_{r_{\text{cir}}}^{r_{\text{LC}}} \frac{\Delta k}{2} dr = \int_{r_{\text{cir}}}^{r_{\text{LC}}} \frac{\Delta n \omega}{2c} dr \simeq \int_{r_{\text{cir}}}^{r_{\text{LC}}} -\frac{v \gamma^{-1} u_r}{1 - u_r^2} \frac{\Delta N}{N} \frac{\omega}{2c} dr, \quad (2.14)$$

where we have assumed  $\beta_{\text{pol}} \sim 0$  since the natural modes are circularly polarized. This integral cannot be evaluated analytically. The most important variable is  $B$ , since  $B \propto r^{-3}$ , and  $v \propto B$ ,  $u_r \propto B$ . The other parameters in the equation do not change or change slowly with  $r$ . Thus, approximately we get

$$\Delta\phi_{\text{PA}} \simeq -\frac{v\gamma^{-1}}{u_r} \frac{\Delta N}{N} \frac{\omega}{2c} r_{\text{cyc}} \int_{r_{\text{cir}}/r_{\text{cyc}}}^{r_{\text{LC}}/r_{\text{cyc}}} \frac{u_r^2}{1-u_r^2} d\left(\frac{r}{r_{\text{cyc}}}\right). \quad (2.15)$$

Suppose  $x = r/r_{\text{cyc}}$ , then  $u_r \simeq x^{-3}$ , and the integration term of eq. (2.15) becomes

$$F_x = \int_{r_{\text{cir}}/r_{\text{cyc}}}^{r_{\text{LC}}/r_{\text{cyc}}} \frac{x^{-6}}{1-x^{-6}} dx. \quad (2.16)$$

As discussed above,  $\Delta n$  changes signs when photon propagates across  $r_{\text{cyc}}$  (where  $x = 1$ ). Then eq. (2.15) becomes

$$\Delta\phi_{\text{PA}} \simeq 0.19\eta P_{\text{ls}}^{-1} B_{*,12}^{1/3} \theta_B^{4/3} \gamma^{-1/3} (\Delta N/N) F_x \nu_9^{-1/3}, \quad (2.17)$$

where  $\eta = N/N_{\text{GJ}}$  is the plasma density parameter,  $P_{\text{ls}} = P/1 \text{ s}$ . Equation (2.17) gives a simple approximate description to the final Faraday rotation angle. It is proportional to  $B_*$ ,  $\eta$ ,  $\Delta N/N$ , but inversely proportional to  $P$ ,  $\gamma$  and  $\nu$ . Notice that  $\Delta\phi_{\text{PA}} \propto \nu_9^{-1/3} \propto \lambda^{1/3}$ , quite different from the FR in ISM (for which  $\Delta\phi_{\text{PA}} \propto \lambda^2$ ). If the plasma is highly symmetrical ( $\Delta N/N \ll 1$ ), since  $\phi_{\text{PA}} \propto \Delta N/N$ , the Faraday rotation is negligible. However, if the plasma is highly asymmetrical, for example,  $\Delta N/N \sim 1$  (the case of pure electrons),  $r_{\text{cir}}/r_{\text{cyc}}$  could be less than 1, the Faraday rotation angle could be significant. For typical parameters of a pulsar magnetosphere,  $B_* = 10^{12} \text{ G}$ ,  $P = 1 \text{ s}$ ,  $\gamma = 100$ ,  $\eta = 1000$ ,  $\Delta N/N \sim 1$ ,  $\theta_B \sim 0.1$ , the circularization radius can be  $r_{\text{cir}}/r_{\text{cyc}} \sim 0.5$ , and the final rotation angle  $\Delta\phi_{\text{PA}} \simeq 0.9\nu_9^{-1/3}$ .

Notice that in our derivation of equations (2.15) and (2.17), the  $\mathbf{k}$ - $\mathbf{B}$  angle  $\theta_B$  is assumed to be a constant in the propagation. In reality,  $\theta_B$  also changes along the photon path. Additionally,  $F_x$  given by eq. (2.16) is related to  $r_{\text{cir}}$  and  $r_{\text{cyc}}$ , both of which are determined by the plasma parameters [see eqs. (2.13) and (2.10)]. Thus, the Faraday rotation angle given in equations (2.15) and (2.17) is only a simple approximation. We will obtain the precise rotation angle by numerical integration of wave evolution equation in § 3.

## 2.2 Evolution of mode amplitude and adiabatic condition

In the  $xyz$  frame [defined with  $\hat{\mathbf{z}} = \hat{\mathbf{k}}$ ,  $\hat{\mathbf{B}} = (-\sin\theta_B, 0, \cos\theta_B)$ ], there are two wave modes: “+” mode and “−” mode. We introduce a mixing angle,  $\theta_m$ , via  $\tan\theta_m = 1/(K_+)$ , so that

$$\tan 2\theta_m = \beta_{\text{pol}}^{-1}. \quad (2.18)$$

In the  $xyz$  frame, the transverse components of the mode eigenvectors are then

$$\mathbf{E}_+ = \begin{pmatrix} i \cos\theta_m \\ \sin\theta_m \end{pmatrix}, \quad \mathbf{E}_- = \begin{pmatrix} -i \sin\theta_m \\ \cos\theta_m \end{pmatrix}. \quad (2.19)$$

In the fixed observers'  $XYZ$  frame [defined by  $\hat{\mathbf{Z}} = \hat{\mathbf{k}}, \hat{\mathbf{\Omega}}$  in the  $XZ$ -plane and  $\hat{\mathbf{k}} \times \hat{\mathbf{\Omega}} = \Omega \sin \zeta \hat{\mathbf{Y}}$ , the direction of  $\mathbf{B}$  in this frame is  $(\theta_B, \phi_B)$ ], they become

$$\mathbf{E}_+ = \begin{pmatrix} i \cos \theta_m \cos \phi_B - \sin \theta_m \sin \phi_B \\ i \cos \theta_m \sin \phi_B + \sin \theta_m \cos \phi_B \end{pmatrix}, \mathbf{E}_- = \begin{pmatrix} -i \sin \theta_m \cos \phi_B - \cos \theta_m \sin \phi_B \\ -i \sin \theta_m \sin \phi_B + \cos \theta_m \cos \phi_B \end{pmatrix}. \quad (2.20)$$

The general wave amplitudes can be written as

$$\begin{pmatrix} A_X \\ A_Y \end{pmatrix} = A_+ \mathbf{E}_+ + A_- \mathbf{E}_-. \quad (2.21)$$

Substitute this into the wave equation, we obtain the mode amplitude evolution equation:

$$i \frac{d}{dr} \begin{pmatrix} A_+ \\ A_- \end{pmatrix} = \begin{bmatrix} -\Delta k/2 + \phi'_B \sin 2\theta_m & i\theta'_m + \phi'_B \cos 2\theta_m \\ -i\theta'_m + \phi'_B \cos 2\theta_m & \Delta k/2 - \phi'_B \sin 2\theta_m \end{bmatrix} \begin{pmatrix} A_+ \\ A_- \end{pmatrix}, \quad (2.22)$$

where the superscript  $(')$  specifies  $d/dr$ ,  $\Delta k = k_+ - k_- = \Delta n \omega / c$ , and a non-essential unity matrix has been subtracted. This equation generalizes the results in special cases (where only  $\theta_m$  or  $\phi_B$  varies) studied in Lai & Ho (2002, 2003) and van Adelsberg & Lai (2006), and therefore is useful for understanding the effect of mode coupling and Faraday rotation.

When the natural modes are circularly polarized, which means  $\theta_m = 45^\circ$ , eq. (2.22) can be simplified to

$$i \frac{d}{dr} \begin{pmatrix} A_+ \\ A_- \end{pmatrix} = \begin{bmatrix} -\Delta k/2 + \phi'_B & i\theta'_m \\ -i\theta'_m & \Delta k/2 - \phi'_B \end{bmatrix} \begin{pmatrix} A_+ \\ A_- \end{pmatrix}. \quad (2.23)$$

The adiabatic parameter is then defined as

$$\Gamma_{\text{ad}} = \left| \frac{\Delta k/2 - \phi'_B}{\theta'_m} \right|. \quad (2.24)$$

Only when  $\Gamma_{\text{ad}} \gg 1$ , the mode evolution is adiabatic, so that the two natural modes can propagate separately and the Faraday rotation can occur. For the non-adiabatic case of  $\Gamma_{\text{ad}} \ll 1$ , the two modes are coupled with each other, the electromagnetic waves do not interact with the medium and the wave polarization states keep unchange.

For the wave propagation in the interstellar medium, the adiabatic condition is very easily satisfied. However, the pulsar magnetosphere is filled with relativistic streaming pair plasma, the condition is only satisfied in some regions. To evaluate the adiabatic condition  $\Gamma_{\text{ad}} \gg 1$  for  $r \gtrsim r_{\text{cir}}$  (or  $\beta_{\text{pol}} \sim 0$ ), we use  $\Delta k = \Delta n \omega / c$ , with  $\Delta n$  given by eq. (2.12), and

$$\phi'_B = F_\phi / r_{\text{LC}} = 2.1 \times 10^{-10} F_\phi P_{1s}^{-1} \text{ cm}^{-1}, \quad (2.25)$$

with

$$F_\phi = \frac{\sin^2 \alpha \cos \zeta - \sin \alpha \cos \alpha \sin \zeta \cos \Psi}{1 - (\cos \alpha \cos \zeta + \sin \zeta \sin \alpha \cos \Psi)^2}. \quad (2.26)$$

Here  $\alpha$  is the inclination angle between the magnetic axis and the rotation axis of a pulsar,  $\zeta$  is the view angle from the rotation axis, and  $\Psi = \Psi_i + \Omega t$  is the pulsar rotation phase. From the definition of  $\theta_m$ , we have

$$\begin{aligned} \theta'_m &= -\frac{1}{2} \sin^2 2\theta_m \beta_{\text{pol}} \frac{\beta'_{\text{pol}}}{\beta_{\text{pol}}} \\ &= 1.1 \times 10^{-11} B_{*12} P_{1s}^{-4} \nu_9^{-1} \left( \frac{r}{r_{\text{LC}}} \right)^{-3} \left( \frac{L_\beta}{r_{\text{LC}}} \right)^{-1} \frac{\sin^2 2\theta_m}{\theta_B^4 \gamma^3 (\Delta N/N - \Delta\gamma/\gamma)}. \end{aligned} \quad (2.27)$$

Here we define  $L_\beta = \beta_{\text{pol}}/\beta'_{\text{pol}}$  which is the scale length of  $\beta_{\text{pol}}$  variation; generally  $L_\beta \sim r$  since  $\beta_{\text{pol}} \propto r^{-6} \theta_B^{-2}$ . In the upper panels of Figure 1, we give some examples for the evolution of the quantities  $\Delta k/2$ ,  $\phi'_B$  and  $\theta'_m$  along the photon ray for different plasma parameters. In the highly symmetrical plasma model (see Fig. 1a), the refractive indices difference  $\Delta n$  is small, and the evolution is non-adiabatic ( $\Delta k/2 \lesssim \phi'_B, \theta'_m$ ). Thus there is no Faraday rotation in this model. On the other hand, for the highly asymmetrical plasma model (see Fig. 1b), the evolution remains adiabatic all the way along the photon path ( $\Delta k/2 \gg \phi'_B, \theta'_m$ ). Therefore we expect that in this (asymmetric) plasma model, Faraday rotation will be generated. Only in some special cases, for example, if a photon propagates through the region where the magnetic fields change signs along the path very quickly,  $\phi'_B$  could be larger than  $\Delta k/2$ , so that the non-adiabatic mode evolution could occur. This “quasi-transverse magnetic field” case was considered by Broderick & Blandford (2009) and Melrose (2010). However, the radio emission we considered in this paper is generated near the tangential direction of the magnetic field line, and magnetic fields in the outer regions do not change sign along the photon path, thus the “quasi-transverse” situation does not occur in pulsar magnetosphere.

### 3 NUMERICAL RESULTS

The analytic description above for the physical process of the Faraday rotation can only give qualitative results under simplified conditions. Here we use the numerical integrations to calculate how radio polarization evolves as the wave propagates through the pulsar magnetosphere. This allows us to obtain the exact values for the rotated polarization angles  $\phi_{\text{PA}}$  and the rotation measure RM.



### 3.1 Single ray evolution

It is generally accepted that pulsar radio emission originates from the open field line region at a few to tens of neutron star radii (e.g. Cordes 1978; Blaskiewicz et al. 1991; Kramer et al. 1997; Kijak & Gil 2003). We assume the emission height  $r_{\text{em}} = 50R_*$  and at the emission point, the photon is polarized in the  $\mathbf{k}$ - $\mathbf{B}$  plane (i.e. the O-mode in the case of curvature radiation) and propagates along the tangential direction of the local field line. We neglect the emission cone of opening angle  $1/\gamma$ . For a given emission height  $r_{\text{em}}$ , pulsar initial rotation phase  $\Psi_i$ , the inclination angle  $\alpha$  (i.e., the  $\boldsymbol{\mu}$ - $\boldsymbol{\Omega}$  angle), the view angle of line of sight  $\zeta$  (i.e., the  $\mathbf{k}$ - $\boldsymbol{\Omega}$  angle), the surface magnetic field  $B_*$ , and the plasma properties (plasma density parameter  $\eta = N/N_{\text{GJ}}$ , Lorentz factor of the streaming plasma  $\gamma$ ), we can numerically calculate the dielectric tensor at each point along the photon ray [see equation (3.15) in WLH10], and integrate the wave evolution equation [given by equation (2.10) in WLH10] from the emission point to a very large radius, which we take the light cylinder radius  $r_{\text{lc}}$ , to determine the final polarization state of the photon.

We first consider magnetospheres consisting of electrons and positrons, with the net charge density given by the Goldreich-Julian model, i.e.,  $N_p - N_e = N_{\text{GJ}}$ . We assume that the total plasma density is  $N = N_p + N_e = 1000N_{\text{GJ}}$ , which means the plasma is almost symmetric for electrons and positrons. Figure 1a shows an example of the photon polarization evolution along its trajectory in such a plasma. The wave natural modes are linearly polarized within the cyclotron absorption radius ( $\sim 1650R_*$ ). Before the cyclotron resonance, the dominated propagation effect is the wave mode coupling (around  $\sim 600R_*$ ), where circular polarization is generated. Although the natural modes become circularly polarized near  $r \simeq 2600R_*$ , the refractive index difference is very small and the mode evolution is non-adiabatic too ( $\Delta k/2 < \phi'_B, \theta'_m$ ); these make the Faraday rotation ineffective. Thus the PA remains unchanged outside the wave mode coupling area of  $\sim 600R_*$  (see the bottom panel of Fig. 1a).

Figure 1b shows the case where the magnetosphere plasma consists of electrons and ions, without positrons at all,  $N = N_e = 1000N_{\text{GJ}}$ ,  $N_p = 0$ . The ions can be neglected for the emission and propagation effects since they are too heavy compared with the electrons. In this case, the adiabatic condition of  $\Delta k/2 > \phi'_B, \theta'_m$  is always satisfied (the upper panel of Fig. 1b). The refractive index difference is also much larger than that for the symmetric case. In the region of  $r < 800R_*$ , the wave mode coupling dominates for the wave propagation.

Farther out, the natural wave modes becomes circularly polarized ( $r_{\text{cir}} \sim 900R_*$ ), Faraday rotation occurs and the direction of linear polarization varies (the bottom panel). Note that at the cyclotron resonance ( $r_{\text{cyc}} \sim 1700R_*$ ),  $\Delta k/2$  changes sign, so the rotation measure changes sign too. The final Faraday rotation angle is about  $20^\circ$ . In Fig. 1c we consider the same case as in Fig. 1b except for the emission coming from the other magnetic pole.

### 3.2 Rotation measure in electron-ion plasma of pulsar magnetosphere

As discussed above, the Faraday rotation effect is negligible in a highly symmetric electron-positron pair plasma of pulsar magnetosphere, while may be significant in an asymmetric plasma, e.g., electron-ion streams. In this subsection, we study the asymmetric case in more detail and present the rotation measure values for various plasma parameters.

In Figure 2, we show some examples of the PA changes for different pulsar and magnetosphere plasma properties, such as different electron density parameter  $\eta = N/N_{\text{GJ}}$  (Fig. 2a), wave frequency  $\nu$  (Fig. 2b), surface magnetic field  $B_*$  (Fig. 2c), pulsar period  $P$  (Fig. 2d), Lorentz factor of plasmas  $\gamma$  (Fig. 2e) and the emission height  $r_{\text{em}}$  (Fig. 2f). In general, the Faraday rotated PA increases with  $\eta$  and  $B_*$ , but decreases with  $\nu$  and  $P$ , and almost does not change with  $\gamma$  and  $r_{\text{em}}$ , roughly in agreement with eq. (2.17).

Interpulses have been detected from a few tens of pulsars (e.g. Weltevrede & Johnston 2008), which is  $180^\circ$  away from the main pulse and comes from the other magnetic pole of a pulsar. In this case, the magnetic fields along the photon trajectory have the opposite directions, and Faraday rotation should have the opposite sign. The PA evolution is also exactly opposite to that for the mainpulse case (see Fig. 1c).

#### 3.2.1 Faraday Rotation Measure

For given pulsar and plasma properties, we can calculate the rotated PA for various frequencies. Note that some other propagation effects, such as wave mode coupling and quasi-tangential effect (see WLH10), can also modify PA unless the modes evolution becomes non-adiabatic or the natural modes become circularly polarized. In general, the final PA value compared with the initial value at emission point is given by

$$\phi_{\text{PA}} = \phi_{\text{other}} + \phi_{\text{FR}}, \quad (3.28)$$

where  $\phi_{\text{FR}}$  is the Faraday rotation angle, and  $\phi_{\text{other}}$  is the rotation angle caused by other propagation effects in the magnetosphere. The Faraday rotation angles have the same mag-

nitude but different signs for the opposite magnetic poles. The other propagation effects, such as wave mode coupling, are the same for the opposite poles. Note that the cyclotron absorption effect will absorb opposite circular polarization but does not affect the linear polarization angle. Therefore we have  $\phi_{\text{PA,opp}} = \phi_{\text{other}} - \phi_{\text{FR}}$  for the emission from the opposite magnetic pole. In general, we can compute  $\phi_{\text{PA}}$  and  $\phi_{\text{PA,opp}}$  using numerical integrations. To eliminate the PA rotation from other propagation effects, we simply use the  $\phi_{\text{PA}}$  value from the two poles to calculate Faraday rotation angle as

$$\phi_{\text{FR}} = (\phi_{\text{PA}} - \phi_{\text{PA,opp}})/2. \quad (3.29)$$

Figure 3 shows how the Faraday rotation angle varies with the wavelength. We find that  $\phi_{\text{FR}}$  is not proportional to  $\lambda^2$  in a pulsar magnetosphere (see the left panel of Fig. 3). For a set of given pulsar and plasma parameters, with surface magnetic field  $B_* = 10^{12}\text{G}$ , the best fit is  $\phi_{\text{FR}} = 0.86 \lambda^{0.47}$  (see the right panel of Fig. 3). The index of 0.47 is different from the theoretical prediction of  $1/3$  in eq. (2.17), probably because of the simplifications of  $F_x$  and  $\theta_B$ . In real observations, we always calculate the RM value by

$$\text{RM} = \frac{d\phi_{\text{FR}}}{d\lambda^2}, \quad (3.30)$$

which varies with  $\lambda$  in pulsar magnetosphere as shown in the middle plane of Figure 3. The higher the observed frequency is, the larger the RM is. Roughly,  $\text{RM} \sim 0.2 \lambda^{-1.53}$  can describe RM dependence of  $\lambda$  rather well. For the observation frequency of  $\nu = 1.4\text{GHz}$  (or  $\lambda \simeq 21\text{cm}$ ), the calculated  $\text{RM} \simeq 2 \text{ rad m}^{-2}$ .

For a higher surface magnetic field,  $B_* = 5 \times 10^{12}\text{G}$ , the Faraday rotated angles are larger compared with those for  $B_* = 10^{12}\text{G}$  (see Fig. 2c and Fig. 3). The relation between  $\phi_{\text{FR}}$  and  $\lambda$  can be fitted to be  $\phi_{\text{FR}} = 2.28 \lambda^{0.56}$ . The corresponding  $\text{RM} \sim 0.64 \lambda^{-1.44}$ . At  $\nu = 1.4\text{GHz}$ ,  $\text{RM} \simeq 6 \text{ rad m}^{-2}$ .

### 3.2.2 Phase resolved Faraday Rotation Measure

Having studied the Faraday rotation angles and RMs for photons propagating through the magnetosphere with given initial pulsar rotation phases, we can now examine the phase resolved Faraday rotation effect. As shown in Fig. 2f, the emission height (much less than the light cylinder radius) does not significantly affect  $\phi_{\text{FR}}$ . Thus, for simplicity, we assume that all emissions of different rotation phases come from the same height, at  $r_{\text{em}} = 50R_*$ . Figure 4 shows examples of the Faraday rotation measure as a function of the pulsar rotation phase. To obtain RM, we integrate the photon polarization evolution across the magnetosphere,

subtract the PA variation caused by other propagation effects, and then get the Faraday rotated angle  $\phi_{\text{FR}}$ ; we repeat this process with a slightly different frequency, and finally obtain RM at each rotation phase. From Fig. 4, we see that the leading part of RMs are smaller than the trailing part. The maximum RM value appears at  $\Psi_i \simeq 8^\circ$ . The RM profiles change only slightly for different impact angles.

#### 4 CONCLUSIONS

Motivated by recent observations of phase-dependent Faraday rotation measures, we have studied the Faraday rotation effect of wave propagation in pulsar magnetospheres when the natural wave modes are circularly polarized. Pulsar magnetosphere is filled with relativistic streaming plasma, the Faraday rotation effect is different from that of the non-relativistic interstellar medium. We analyzed the wave modes and Faraday rotation effect considering the adiabatic evolution conditions. We used numerical integration of the polarization vector along the photon ray to incorporate all the propagation effects self-consistently within a single framework. We find that for highly symmetric pair plasma, with  $|N_p - N_e| \ll N = N_p + N_e$ , the magnetosphere Faraday rotation is negligible. For asymmetric plasmas (e.g., an electron-ion streams with  $N_e \gg N_{\text{GJ}}$ ), the magnetosphere Faraday rotation effect may be significant. For such an electron-ion plasma of pulsar magnetosphere, the Faraday rotation angle  $\phi_{\text{FR}}$  is not proportional to  $\lambda^2$  in pulsar magnetospheres, but approximately to  $\lambda^{0.5}$ . The induced value of  $\text{RM} \propto \lambda^{-1.5}$ , becomes larger for higher frequencies. The phase resolved RMs have smaller values for leading part and larger values for trailing part. There exists a maximum RM at the trailing half of the emission beam. The RM profiles do not change significantly for various impact angles. The induced rotation measures for the mainpulse and interpulse have the same magnitude but opposite sign.

Our calculations in this paper have relied on several simplified assumptions. For example, we have assumed a cold streaming plasma with the Lorentz factor  $\gamma$  and the density parameter  $N/N_{\text{GJ}}$  constant throughout the magnetosphere. Note that in reality, even when the Faraday rotation effect is very weak for a symmetric pair plasma, other propagation effects can modify the PA curve significantly (see Wang, Lai & Han 2010; Andrianov & Beskin 2010; Beskin & Philippov 2011). Overall, our result shows that an unambiguous identification of the magnetosphere Faraday rotation in the PA data may provide a valuable probe of the physical condition of pulsar magnetospheres.

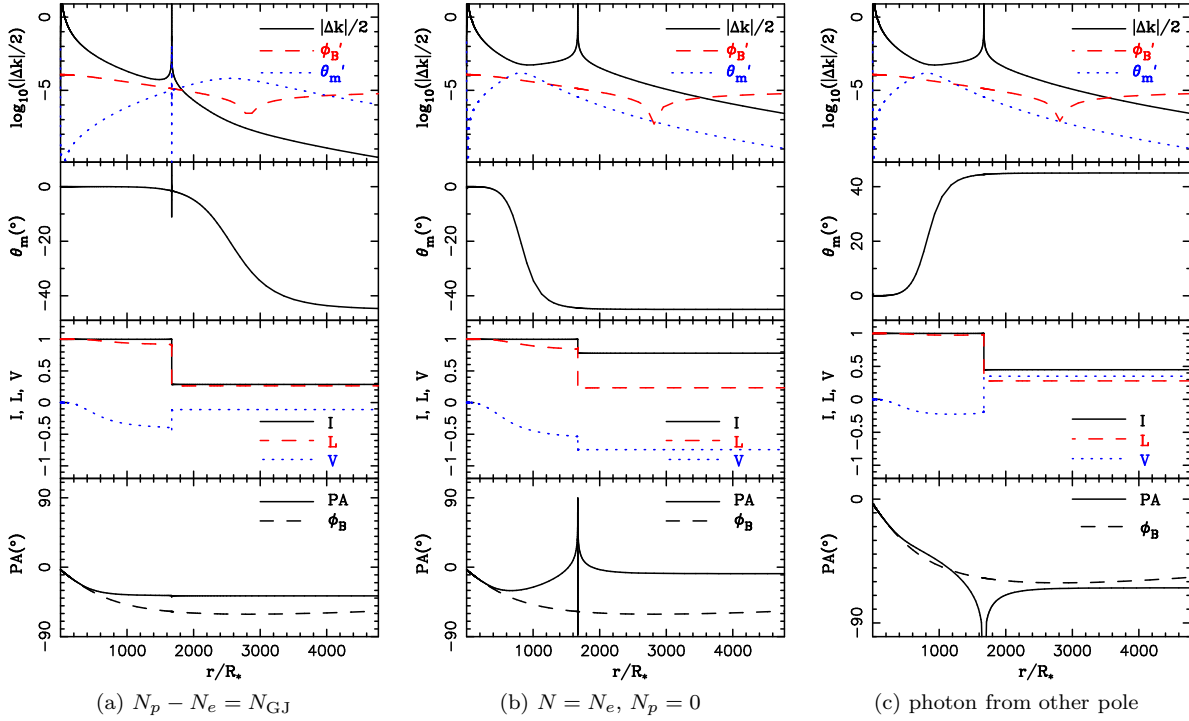


**Figure 1.** Single photon evolutions across the pulsar magnetosphere with the plasma density parameter  $\eta = N/N_{\text{GJ}} = 1000$  and the Lorentz factor  $\gamma = 100$  for a pulsar with surface magnetic field  $B_* = 10^{12}$  G and spin period  $P = 1$  s. The magnetic inclination angle is  $\alpha = 30^\circ$  and the impact angle is  $\chi = \zeta - \alpha = 5^\circ$ . The calculations were made for the wave frequency  $\nu = 1$  GHz, initial rotation phase  $\Psi_i = 0^\circ$ , and emission height  $r_{\text{em}} = 50R_*$ . Panel (a) is for the pair plasma with  $N_p - N_e = N_{\text{GJ}}$ . Panel (b) is the case for the magnetosphere plasma consisting of electrons and ions (without positrons),  $N = N_e$ ,  $N_p = 0$ . Panel (c) is almost the same as panel (b) but for the emission of the opposite magnetic pole.

## ACKNOWLEDGMENTS

This work has been supported by the National Natural Science Foundation of China (11003023, 10773016, 10821061 and 10833003).

## REFERENCES

- Andrianov, A.S., & Beskin, V.S. 2010, *Astron. Lett.*, 36, 248
- Arons, J. & Barnard, J. J. 1986, *ApJ*, 302, 120
- Beskin, V.S., & Philippov, A.A. 2011, *MNRAS*, submitted (arXiv:1101.5733)
- Blaskiewicz, M., Cordes, J. M. & Wasserman, I. 1991, *ApJ*, 370, 643
- Broderick, A. E., & Blandford, R. D. 2010, *ApJ*, 718, 1085
- Cordes, J. M. 1978, *ApJ*, 222, 1006
- Goldreich, P. & Julian, W. H. 1969, *ApJ*, 157, 869
- Hamilton, P. A. & Lyne, A. G. 1987, *MNRAS*, 224, 1073
- Han, J. L., Manchester, R. N., Xu, R. X., & Qiao, G. J. 1998, *MNRAS*, 300, 373
- Han, J. L., Manchester, R. N., Lyne, A. G., Qiao, G. J., & van Straten, W. 2006, *ApJ*, 642, 868
- Karastergiou A., 2009, *MNRAS*, 392, L60
- Kazbegi, A. Z., Machabeli, G. Z. & Melikidze, G. I. 1991, *MNRAS*, 253, 377
- Kennett, M. & Melrose, D. 1998, *PASA*, 15, 211
- Kijak, J. & Gil, J. 2003, *A&A*, 397, 969

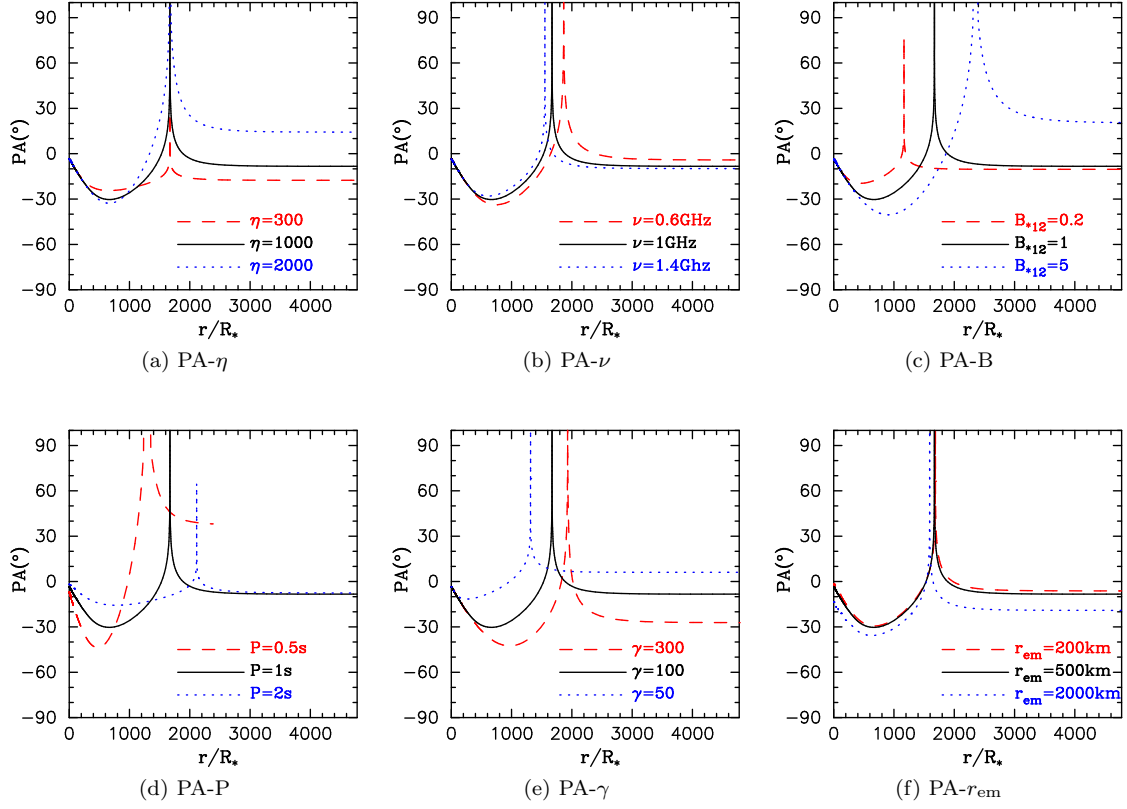


**Figure 2.** The evolution of PA along the photon ray for various pulsar and magnetosphere plasma properties, including density  $\eta = N/N_{GJ}$  (panel a), frequency (panel b), surface B field (panel c), rotation period (panel d), Lorentz factor (panel e) and initial emission height (panel f). In each panel, only one parameter is varied and labeled, while other parameters are the same as those used in Fig. 1b.

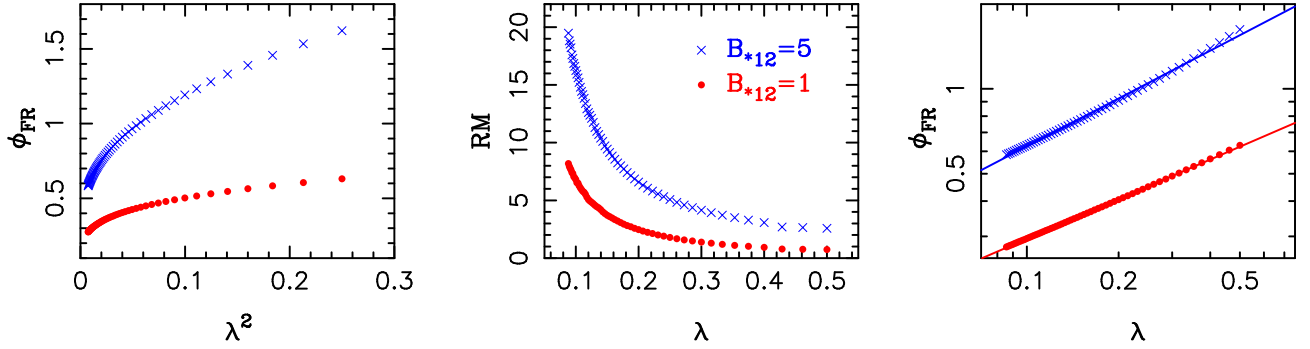


**Figure 3.** The Faraday rotated angle produced in the magnetosphere as a function of the wavelength for  $B_* = 10^{12} \text{G}$  (“•”) and  $B_* = 5 \times 10^{12} \text{G}$  (“×”). The left panel shows  $\phi_{FR}$  against  $\lambda^2$  and the middle panel shows  $RM$  ( $=d\phi_{FR}/d\lambda^2$ ) against  $\lambda$ . The right panel shows the possible relation between  $\log_{10}(\phi_{FR})$  and  $\log_{10}(\lambda)$ , and the two solid lines are  $\phi_{FR} = 0.86 \lambda^{0.47}$  for  $B_* = 10^{12} \text{G}$  and  $\phi_{FR} = 2.28 \lambda^{0.56}$  for  $B_* = 5 \times 10^{12} \text{G}$ . The pulsar and plasma parameters are the same as used in Figure 1b, except for the varying frequencies.

Kramer, M., Xilouris, K. M., Jessner, A., Lorimer, D. R., Wielebinski, R. & Lyne, A. G., 1997, A&A, 322, 846

Lai, D. & Ho, W. C. G. 2003, ApJ, 588, 962

Lai, D. & Ho, W. C. G. 2002, ApJ, 566, 373

Melrose, D. B. 2010, ApJ, 725, 1600

Noutsos, A., Karastergiou, A., Kramer, M., Johnston, S., & Stappers, B.W. 2009, MNRAS, 396, 1559

Ramachandran, R., Backer, D. C., Rankin, J. M., Weisberg, J. M., & Devine, K. E. 2004, ApJ, 606, 1167

Thomson, R. C. & Nelson, A. H. 1980, MNRAS, 191, 863

van Adelsberg, M. & Lai, D. 2006, MNRAS, 373, 1495

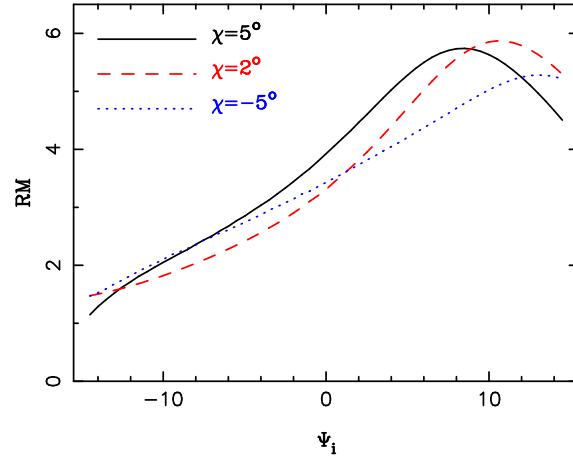


**Figure 4.** Phase resolved RM from pulsar magnetospheres for different impact angles of  $\chi = 5^\circ$  (solid line),  $2^\circ$  (dashed line) and  $-5^\circ$  (dotted line). The pulsar and plasma parameters for the calculation are the same as used in Figure 1b, except for different initial rotation phase  $\Psi_i$  and surface B field  $B_* = 5 \times 10^{12} \text{G}$ .

Wang, C. & Lai, D. 2007, MNRAS, 377, 1095

Wang, C., Lai, D., & Han, J. L. 2010, MNRAS, 403, 569

Weltevrede, P. & Johnston, S. 2008, MNRAS, 387, 1755